The Journal of Chemical Physics

Calculation and analysis of the harmonic vibrational frequencies in molecules at extreme pressure: Methodology and diborane as a test case

Cite as: J. Chem. Phys. **137**, 154112 (2012); https://doi.org/10.1063/1.4757285
Submitted: 10 July 2012 . Accepted: 19 September 2012 . Published Online: 19 October 2012

R. Cammi, C. Cappelli, B. Mennucci, and J. Tomasi

AIP Publishing

Calculation and analysis of the harmonic vibrational frequencies in molecules at extreme pressure: Methodology and diborane as a test case

R. Cammi,[1,a)] C. Cappelli,[2,3] B. Mennucci,[2] and J. Tomasi[2]
[1]*Dipartimento di Chimica, Università di Parma, Viale Parco Area delle Scienze 17/A, I-43100 Parma, Italy*
[2]*Dipartimento di Chimica e Chimica Industriale, Università di Pisa, via Risorgimento 35, I-56126 Pisa, Italy*
[3]*Scuola Normale Superiore, Piazza dei Cavalieri 7, I-56126 Pisa, Italy*

(Received 10 July 2012; accepted 19 September 2012; published online 19 October 2012)

We present a new quantum chemical method for the calculation of the equilibrium geometry and the harmonic vibrational frequencies of molecular systems in dense medium at high pressures (of the order of GPa). The new computational method, named PCM-XP, is based on the polarizable continuum model (PCM), amply used for the study of the solvent effects at standard condition of pressure, and it is accompanied by a new method of analysis for the interpretation of the mechanisms underpinning the effects of pressure on the molecular geometries and the harmonic vibrational frequencies. The PCM-XP has been applied at the density functional theory level to diborane as a molecular system under high pressure. The computed harmonic vibrational frequencies as a function of the pressure have shown a satisfactory agreement with the corresponding experimental results, and the parallel application of the method of analysis has reveled that the effects of the pressure on the equilibrium geometry can be interpreted in terms of direct effects on the electronic charge distribution of the molecular solutes, and that the effects on the harmonic vibrational frequencies can be described in terms of two physically distinct effects of the pressure (*curvature* and *relaxation*) on the potential energy for the motion of the nuclei. © *2012 American Institute of Physics*. [http://dx.doi.org/10.1063/1.4757285]

I. INTRODUCTION

In a previous paper of some of the present authors[1] we presented a quantum mechanical (QM) method to study the properties of molecular systems within a medium at high pressure regime (of the order of GPa). The method (called PCM-XP) is based on an adaptation of the polarizable continuum model (PCM), developed by our group[2–6] for the study of molecules in solution. PCM codes have been well tested and amply used to study a large variety of properties at the standard conditions of pressure ($p = 1$ bar $= 10^{-4}$ GPa) and temperature. In this paper we present an extension of the PCM-XP method to study the effect of the pressure on the harmonic vibrational frequencies of molecular systems in dense phases. This extension of the PCM-XP model is mainly motivated by the interest toward applications to experimental observables, which in dense material at high pressure are primarily of spectroscopic nature,[7–10] and in particular of vibrational type.[11–21]

The physics underlying the PCM-XP model accounts for the fact that the primary action of the pressure,[22,23] at high regimes, consists in reducing the intermolecular distances below to the van der Waals values, so allowing the penetration into the region of intermolecular potentials dominated by the Pauli repulsive interaction.[24–27]

The basic version of the PCM-XP model describes the effect of the high pressure molecular properties in the following way. The environment is represented by a continuum medium hosting a QM solute into a molecularly shaped cavity. The medium is characterized in terms of its dielectric permittivity and of its averaged electronic charge distribution. The electronic distribution of the medium is treated as an uniform continuum defined outside the cavity hosting the solute, and with density equal to the valence electron distribution of the bulk environment at the given pressure condition.

The Pauli repulsion between the molecule and the external medium is described in terms of the overlap between the charge distribution of the solute and the charge distribution of the solvent in the region outside the molecular cavity. The analytical form of this interaction exploits a generalization to the PCM model of the expressions used within the framework of the molecular interaction theory.[28] The Pauli repulsion contribution is inserted into a suitable basic energy functional to be minimized in the QM procedure for the determination of the electronic wavefunction of the molecular solute.[28] The QM basic energy functional also acts as source for the potential energy surfaces ruling the nuclear motion within the Born-Oppenheimer approximation.

The primary action of the pressure (i.e., the increase of the Pauli repulsion) is modeled by shrinking the cavity volume with respect to its reference value corresponding to the standard conditions of pressure ($p = 1$ bar). This shrinking determines an increase of amount the electronic charge density that lies outside of the cavity and overlaps with the charge distribution of the solvent, with a consequent corresponding increase of the Pauli repulsion.

The pressure is then determined as the first derivative of the QM basic energy functional with respect to the volume of

a)Author to whom correspondence should be addressed. Electronic mail: roberto.cammi@unipr.it. Telephone: +39-0521-905442. Fax: +39-0521-905557.

the cavity, and other first order derivatives of the same QM functional are exploited for the evaluation of the stationary point of the PES corresponding to the equilibrium geometries, and for the determination of the first-order properties of the solute at the given condition of the pressure.

The extension of the basic PCM-XP model for the harmonic vibrational frequencies at high pressure touches all the key aspects of the corresponding PCM calculations at the standard condition of pressure.[29] In that case, the vibrational harmonic frequencies and the corresponding normal modes of the solvated molecules are computed from the second derivatives of the basic free energy functional (only including the electrostatic components of the solute-solvent interaction) with respect to the Cartesian coordinates, computed at the equilibrium geometry in solution. A nonequilibrium solvation approach is adopted for the description of the vibrational frequencies of solvated molecules. The nonequilibrium solvation accounts for the dynamical aspects of the solvent polarization, and in the common practice it is assumed that the geometry of the molecular cavity does not follow the solute vibrational motion.[30] The second derivatives of the QM free energy functional are determined by a suitable analytical algorithm detailed in Ref. 31, which allows a computational effort for the calculation of the vibrational properties in solution similar to that for the corresponding calculation in the gas phase. However, in the current implementations the QM free-energy functional is limited to the electrostatic components of the solute solvent-interaction.

Passing to the study of harmonic vibrational frequencies of molecules at high pressure, the new aspect to take into account is the presence of the Pauli repulsion between the molecular systems and the environment, which requires an extension of the analytical second derivatives for QM free energy functional.

The purpose of this paper is not limited to present effective computational tools for the determination of the harmonic vibrational frequencies of molecules at high-pressure. In a systematic research effort regarding the calculation of molecular observables in a dense phase,[32] the elaboration of a formal theoretical approach to follow, and its translation into a computational code are only the initial steps of this effort. To these steps others must follow: (i) the selection of an appropriate hierarchy of QM computational levels, (ii) the collections of an adequate number of numerical results, and (iii) the analysis of the numerical results paying particular attention to the possible occurrence of phenomena not put in evidence in preceding studies. For this methodological reason, in this paper we also present an adequate theoretical scheme for the analysis of the computational outcomes of the effects of the pressure on the equilibrium geometry and on harmonic vibrational frequencies.

The paper is organized as follows. In Sec. II we review the basic aspects of the PCM-XP model, and we present the theory of its first analytical second derivatives; in Sec. III we detail the computational protocol to perform the PCM-XP calculations; finally, in Sec. IV we present a numerical application to the calculation and analysis of the harmonic vibrational frequencies of diborane within the range of pressures 1–25 GPa.

II. THEORY

In this section, we review the basic theory of PCM-XP model presented in Ref. 1, and we present the theory for the analytical second derivatives required for the calculation of the harmonic vibrational frequencies.

A. The basic PCM-XP: Hamiltonian, energy functional, and pressure

The properties of molecules within a dense environment at high pressure are determined by solving the Schrödinger equation for the effective nonlinear Hamiltonian:

$$\hat{H} = \hat{H}^o + \hat{V}_{int}(\Psi), \tag{1}$$

being H^o is the Hamiltonian of the isolated molecule and $\hat{V}_{int}(\Psi)$ the molecule-environment interaction operator given by

$$\hat{V}_{int}(\Psi) = \hat{V}_e(\Psi) + \hat{V}_r. \tag{2}$$

Here $\hat{V}_e(\Psi)$ and $\hat{V}_r$ are, respectively, the usual PCM electrostatic interaction term and the non-electrostatic Pauli repulsion contribution, and the argument of $\hat{V}_e(\Psi)$ denotes its dependence on the wavefunction $\Psi >$ of the molecular solute.[6]

In the computational practice, $\hat{V}_e(\Psi)$ is represented in terms of a set of polarization point charges located at the cavity surface, and it may be written as

$$\hat{V}_e(\Psi) = \bar{\mathbf{Q}}(\Psi) \cdot \hat{\mathbf{V}}, \tag{3}$$

where $\bar{\mathbf{Q}}(\Psi)$ is a vector collecting the set of polarization charges induced by the charge distribution of solute, $\hat{\mathbf{V}}$ is a vector operator representing the electrostatic potential of the solute at the boundary of the cavity, and the dot represents an inner product. The solvent polarization charges $\bar{\mathbf{Q}}(\Psi)$ depend on the wavefunction of the solute as expectation value $\bar{\mathbf{Q}}(\Psi) = \langle\Psi|\hat{\mathbf{Q}}|\Psi\rangle$ of a suitable apparent charge operator $\hat{\mathbf{Q}}$.[33] There are several definitions of the $\hat{\mathbf{Q}}$ operator according to the several variants of the PCM method.[6] Here we refer to the most general variant, the integral equation formalism version (IEF-PCM).[4,35–39]

The Pauli repulsion operator $\hat{V}_r$ of Eq. (2) has the nature of a repulsive step potential located at the boundary of the cavity, and it has the structure of a pseudo-integral operator with kernel:[34]

$$\hat{V}_r(\mathbf{r}) = \hat{\rho}(\mathbf{r})H(\mathbf{r}), \tag{4}$$

where $\hat{\rho}(\mathbf{r}) = \sum_i^N \delta(\mathbf{r} - \mathbf{r}_i)$ is the electron density operator (over the N electrons of the molecular system), and $H(\mathbf{r})$ is a step barrier potential:

$$H(\mathbf{r}) = V_0\Theta(\mathbf{r}) \qquad \Theta(\mathbf{r}) = \begin{cases} 1 & \mathbf{r} \subseteq \mathbf{C} \\ 0 & \mathbf{r} \nsubseteq \mathbf{C} \end{cases}, \tag{5}$$

where $\Theta(\mathbf{r})$ is a Heaviside step function located at the boundary of the cavity, and V_0 is the height of the potential barrier, given by

$$V_0 = \gamma n_S. \tag{6}$$

The two quantities γ and n_S appearing in the definition (6) of the barrier height are, respectively, a semiempirical parameter

and the numeral density of the valence electron of the external medium, both depending on the given condition of pressure. They will be better defined in the Sec. III.

The basic energy functional to be minimized during the QM procedure has the thermodynamic status of a free-energy for the whole molecule-environment system, and is defined as

$$G_{e-r} = \langle \Psi | \hat{H}^o + \frac{1}{2}\bar{\mathbf{Q}}(\Psi) \cdot \hat{\mathbf{V}} + \hat{V}_r | \Psi \rangle + \tilde{V}_{nn}, \qquad (7)$$

where $\tilde{V}_{nn}$ is the nuclei-nuclei interaction contribution in the presence of the external medium. The reference state for G_{e-r} is given by a hypothetical state composed by the non-interacting electron and nuclei of the solute, and by the unperturbed medium at the chosen thermodynamic conditions.[40]

The free energy functional G_{e-r} can be written in the following matrix form:

$$G_{e-r} = \left[tr\mathbf{Ph} + \frac{1}{2} tr\mathbf{PG}(\mathbf{P}) \right] + tr\mathbf{Ph}^e + \frac{1}{2} tr\mathbf{PX}^e(\mathbf{P}) + tr\mathbf{Ph}^r + \tilde{V}_{nn}, \qquad (8)$$

where the approximation of using a one-determinantal description of the electronic wavefunction of the solute, with a basis set expansion of the molecular orbitals, is assumed. In Eq. (8), the **P** matrix describes, within the given basis set, the one-electron distribution of the solute, and the terms within the square brackets correspond to usual one-electron **h** and two-electron **G**(**P**) contributions of the isolated molecule energy. The matrices $\mathbf{h}^e$ and $\mathbf{X}^{el}(\mathbf{P})$ collect, respectively, one- and two-electron integrals describing the electrostatic interaction with the solvent, and the matrix $\mathbf{h}^r$ collects the one-electron integrals representing the repulsion operator $\hat{V}_r$ of Eq. (4). The elements of all the matrices are the sum of integrals referring each to the representative point of a tessera of the cavity surface. We refer to the quoted paper[1] for more details, we limit to consider the explicit expression for the elements of matrix $\mathbf{h}^r$:

$$h^r_{\mu\nu} = V_0 \langle \chi_\mu | v_r | \chi_\nu \rangle, \qquad (9)$$

where v_r is a one-electron integral operator with kernel $v_r(\mathbf{r}) = \delta(\mathbf{r} - \mathbf{r}')\Theta(\mathbf{r})$. In computational practice, the matrix elements $h^r_{\mu\nu}$ are evaluated exploiting the Gauss theorem[41] of classical electrostatics, to obtain the following expression:[28]

$$h^r_{\mu\nu} = V_0 \left(S_{\mu\nu} - S^{in}_{\mu\nu} \right), \qquad (10)$$

where $S_{\mu\nu}$ is a matrix element of the overlap matrix over the expansion basis set and $S^{in}_{\mu\nu}$ is given by

$$S^{in}_{\mu\nu} = \frac{1}{4\pi} \sum_k a_k \mathbf{E}_{\mu\nu}(\mathbf{s}_k) \cdot \mathbf{n}_k(\mathbf{s}_k), \qquad (11)$$

with the summation running over the tessera. The elements a_k, $\mathbf{E}_{\mu\nu}(\mathbf{s}_k)$, $\mathbf{n}_k(\mathbf{s}_k)$ are, respectively, the area of the kth tessera, a matrix element of the electric field integrals evaluated at the representative point $\mathbf{s}_k$, and the unit vector normal to the tessera at the same point.

The free-energy functional of Eq. (8) subjected to the stationarity conditions leads to the Fock matrix for the molecular solute:

$$F_{\mu\nu} = \frac{\partial G_{e-r}}{\partial P_{\mu\nu}} = \left(h_{\mu\nu} + h^e_{\mu\nu} + h^r_{\mu\nu} \right) + G_{\mu\nu}(\mathbf{P}) + X^e_{\mu\nu}(\mathbf{P}). \qquad (12)$$

The molecular orbitals (MOs) calculated from the Fock matrix (12), and any other properties of the target molecules, must be related to the pressure p.

The pressure is a macroscopic thermodynamic property that can be connected by a suitable choice of a statistical ensemble to QM methods addressing to the description of a single molecule. Within the PCM-XP model, the choice of a canonical ensemble approach[42,43] leads to the following equation:[44,45]

$$p = -\left(\frac{\partial G_{e-r}}{\partial V_c} \right), \qquad (13)$$

where V_c is volume of the cavity hosting the molecule. We remark that, with respect to the more simple QM models based on impenetrable potential wall,[47–54] the nature of QM Pauli repulsion contribution to the PCM free-energy functional G_{e-r} allows a confinement of the electronic charge distribution of the solute in a smooth way. See, on this point, the concluding remarks of Le Sar and Herschbach in their seminal paper.[49]

As already said in the Introduction, the first- and higher order molecular properties of the molecular solute at a given pressure p can be expressed as a suitable derivatives of the corresponding free energy functional G_{e-r}.

B. The analytical gradients

The first derivative of the free-energy functional (8) with respect to a given parameter α may be written as

$$G^\alpha_{e-r} = tr\mathbf{Ph}^\alpha + \frac{1}{2} tr\mathbf{PG}^\alpha(\mathbf{P}) + tr\mathbf{Ph}^{e,\alpha} + \frac{1}{2} tr\mathbf{PX}^{e,\alpha}(\mathbf{P}) + tr\mathbf{Ph}^{r,\alpha} - tr\mathbf{S}^\alpha\mathbf{W} + \tilde{V}^\alpha_{nn}, \qquad (14)$$

where $\mathbf{W} = \mathbf{PFP}$ is the energy-weighted density matrix, and the upper script α denotes the first derivatives of the pertinent entity (e.g., $\mathbf{S}^\alpha$ is the first derivative of the overlap matrix). We refer again to the quoted papers for more details on the derivatives of electrostatic matrices $\mathbf{h}^{e,\alpha}$ and $\mathbf{X}^{e,\alpha}(\mathbf{P})$. The derivative matrix of the QM Pauli repulsion term $\mathbf{h}^{r,\alpha}$ of Eq. (14) has elements:

$$h^{r,\alpha}_{\mu\nu} = V_0 \left(S^\alpha_{\mu\nu} - S^{in,\alpha}_{\mu\nu} \right), \qquad (15)$$

with the matrix elements $S^{in,\alpha}_{\mu\nu}$ given by

$$h^{r,\alpha}_{\mu\nu} = V_0 \left[S^\alpha_{\mu\nu} + \frac{1}{4\pi} \sum_k \left[\mathbf{E}_{k,\mu\nu} \cdot \left(\mathbf{n}^\alpha_k a_k + \mathbf{n}_k a^\alpha_k \right) + \left(\mathbf{E}^\alpha_{k,\mu\nu} + \mathbf{s}^\alpha_k \cdot \nabla \mathbf{E}_{k,\mu\nu} \right) \cdot \mathbf{n}_k a_k \right] \right], \qquad (16)$$

where $\mathbf{E}^\alpha_{k,\mu\nu}$ is the derivative of the basis functions in the matrix elements of the electric field operator, while $\mathbf{n}^\alpha_k$ and a^α_k are, respectively, the derivative of the unit normal vector and of the area of the kth tessera, and $\nabla \mathbf{E}_{k,\mu\nu}$ is the matrix of the

electric field gradient operator at the representative point $\mathbf{s}_k$ on the cavity surface.

C. Analytical second derivatives

In this section we present the analytical second derivatives of the free energy functional required for the calculation of the harmonic vibrational frequencies. As anticipated in the Introduction, the geometrical derivatives will be considered within a non-equilibrium solvation regime, which assumes a fixed geometry for the cavity.

The direct differentiation of the analytical gradient (14) leads to the analytical second derivative of the basic energy functional (8) with respect to parameters α and β:

$$G_{e-r}^{\alpha\beta} = tr\mathbf{P}\mathbf{h}^{\alpha\beta} + \frac{1}{2}tr\mathbf{P}\mathbf{G}^{\alpha\beta}(\mathbf{P}) + tr\mathbf{P}\mathbf{h}^{e,\alpha\beta} + \frac{1}{2}tr\mathbf{P}\mathbf{X}^{e,\alpha\beta}(\mathbf{P}) + tr\mathbf{P}\mathbf{h}^{r,\alpha\beta} + tr\mathbf{P}^{\alpha}\mathbf{F}^{[\beta]}(\mathbf{P}) - tr\mathbf{S}^{\alpha\beta}\mathbf{W} - tr\mathbf{S}^{\alpha}\mathbf{W}^{\beta}, \tag{17}$$

where $\mathbf{P}^{\beta}$ and $\mathbf{W}^{\beta}$ are, respectively, the derivatives of the one-particle density matrix and of the energy weighted density matrix; $\mathbf{F}^{[\beta]}(\mathbf{P})$ collects the partial derivatives of the Fock matrix:

$$\mathbf{F}^{[\beta]}(\mathbf{P}) = \mathbf{h}^{\beta} + \mathbf{h}^{e,\beta} + \mathbf{h}^{r,\beta} + \mathbf{G}^{\beta}(\mathbf{P}) + \mathbf{X}^{e,\beta}(\mathbf{P}). \tag{18}$$

The other terms of Eq. (17) involve first and second derivatives of the AO matrix elements. The specific expression for the second derivative of the Pauli repulsion contribution is given by

$$h_{\mu\nu}^{r,\alpha\beta} = V_0\left(S_{\mu\nu}^{\alpha\beta} + \frac{1}{4\pi}\sum_k \mathbf{E}_{k,\mu\nu}^{\alpha\beta}\cdot\mathbf{n}_k a_k\right) \tag{19}$$

where $\mathbf{E}_{k,\mu\nu}^{\alpha\beta}$ denotes a second derivative of the AO basis functions in electric field integrals $\mathbf{E}_{k,\mu\nu}$.

The first derivative of energy weighted density matrix $\mathbf{W}^{\beta}$ is

$$\mathbf{W}^{\beta} = \mathbf{P}^{\beta}\mathbf{F}\mathbf{P} + \mathbf{P}\mathbf{F}^{\beta}\mathbf{P} + \mathbf{P}\mathbf{F}\mathbf{P}^{\beta}, \tag{20}$$

where $\mathbf{F}^{\beta}$ is the total derivative of the Fock matrix:

$$\mathbf{F}^{\beta} = \mathbf{F}^{[\beta]} + \mathbf{G}(\mathbf{P}^{\beta}) + \mathbf{X}(\mathbf{P}^{\beta}). \tag{21}$$

The required first derivative of the density matrix $\mathbf{P}^{\beta}$ is obtained by exploiting the coupled-perturbed Hartree-Fock (or Kohn-Sham) procedure within the PCM framework.[55]

We recall that when the parameters α and β correspond to Cartesian coordinates of atomic nuclei, the second derivative of Eq. (17) determines the Hessian matrix from which the harmonic vibrational frequencies and normal modes of the molecules at the high pressure can be obtained. In parallel, when the couple α, β regards the combination of a Cartesian coordinate with a static electric field component, the second derivative (17) contributes to the determination of the IR intensities associated to the vibrational fundamental transitions.[29]

III. COMPUTATIONAL PROTOCOL

To compute the basic energy functional G_{e-r} of the PCM-XP model and its derivatives we need to redefine some of the physical parameters used in the standard PCM calculations: the dimension of the cavity, the dielectric permittivity, ϵ, of the medium, its numeral density, n_S, and the amplitude, V_0, of the Pauli barrier step potential defined in Eq. (6).

A. The molecular cavity: The scaling factor *f*

The reduction of the volume of the cavity hosting the molecular solute determines the increase of the pressure. The cavity is build-up from a set of primary atomic spheres centered on the nuclei of the constituting atoms, and with radii R equal to the corresponding atomic van der Waals radii times a scaling factor f, i.e., $R_i = R_{wdW}f$. The value $f = 1.2$ is usually used for PCM calculations at the standard condition of pressure, in absence of the Pauli repulsive interaction, and this value is here used as an upper limit of the scaling factor f. A lower value of the scaling factor f shrinks the cavity size, determining an increase of the pressure. Numerical tests (see Sec. IV A) show that the range of values $f = 1.2$–0.95 allows to span the range of pressure 1–25 GPa.

A further point regards the finer aspects of the cavity shape. Simple physical arguments suggest the use a solvent excluding surface (SES) cavity topology[6] which introduces additional spheres to take into account the space not available to the solvent molecules. To determine the SES cavity, a solvent molecular probe modelled as a hard sphere of given radius (R_{solv}) is used. In the PCM-XP protocol, the radius of the probe is modified accordingly to the scaling factor f used for the cavity

$$R_{solv} = R_{solv}^0 \cdot f/f_0, \tag{22}$$

where R_{solv}^0 is the probe radius of the external medium at standard condition of pressure, and $f_0 = 1.2$ is the reference cavity scaling factor.

B. The medium properties: Dielectric permittivity and the numeral density

The medium properties as molecular radius R_{solv}, numeral density n_S, and dielectric permittivity ϵ are assumed as functions of the cavity scaling factor f. In fact, as shown in Eq. (23), the scaling factor f is also applied to the molecular radius R_{solv} of the medium, and therefore it corresponds to a linear scaling of the total system (molecule-external medium).[56]

The valence electron density $n_S = n_S(f)$ of the external medium is given as a function of the scaling factor f as

$$n_S(f) = n_S^0(f_0/f)^3, \tag{23}$$

where n_S^0 is the numeral density of the external medium at standard condition of pressure, $f_0 = 1.2$ is the reference cavity scaling factor, and f is the actual cavity scaling factor $f < f_0$.

The dielectric permittivity $\epsilon(f)$ is given by

$$\epsilon(f) = 1 + (\epsilon_0 - 1)(f_0/f)^3, \tag{24}$$

where ϵ_0 is the dielectric permittivity of the medium at the standard pressure condition. The functional form (24) can be derived from the Onsager equation[57,58] for the dielectric permittivity, by assuming the polarizability of the medium molecules (for the sake of simplicity, we consider a non-polar external medium) to be pressure independent.

C. The repulsive step potential: $V_0(N)$

The barrier potential V_0 of Eq. (6) depends on the scaling factor through the numeral density $n_S(f)$ and the semi-empirical parameter γ. As discussed in the Appendix, a convenient functional form for γ is

$$\gamma_N(f) = \gamma_0(f_0/f)^N, \tag{25}$$

where γ_0 is constant ($\gamma_0 = 4\pi/0.7E_h a_o^3$) as detailed in Ref. 28, and the exponent N can be estimated from the pV experimental data of the external medium. Reasonable choices of the parameter N are with the range $N = 3$–6. Introducing Eq. (25) into Eq. (6) we obtain the following explicit form for the barrier eight potential V_0:

$$V_0(N) = \gamma_N(f)n_s(f), \tag{26}$$

where the argument N denotes a parametrical dependence. The higher is the parameter N, the harder is the Pauli barrier potential of the medium.

D. The geometry optimization and the calculation of the harmonic vibrational frequencies

The equilibrium geometries of the molecular solutes have been optimized as a function of the pressure. All the optimizations have been performed with the fixed cavity approximation, which allows the relaxation of the nuclei position but not that of the centers of the spheres. A step-by-step procedure has been exploited. The first step consists in the geometry optimization for the largest cavities (i.e., with factor $f_0 = 1.2$), performed starting from the equilibrium geometry of the solute in the gas phase. The second step is the analogous: geometry optimization within the cavity with scaling factor $f = 1.1$ starting from the equilibrium geometry at f_0. The following steps exploit the same procedure progressively reducing the value of f until the desired value.

The harmonic vibrational frequencies have been determined still maintaining the fixed cavity approximation using the Hessian matrix of second derivatives of Eq. (17) computed at the optimized geometries. This procedure assures that the harmonic frequencies are computed in correspondence to a stationary point of the potential energy surface of the molecular solute.

IV. NUMERICAL RESULTS AND ANALYSIS

Analytical first and second derivatives G^{α}_{e-r} and $G^{\alpha\beta}_{e-r}$ have been implemented into a local version of the GAUSSIAN 09 suite of programs,[59] and, in this section, we present the results of their application to the study of the pressure effects on the harmonic vibrational frequencies of diborane (see Fig. 1). The choice of diborane is related to the availability of experimental IR/Raman spectra within the range of pressures 1–25 GPa,[20,21] which can be compared with numerical results obtained with our PCM-XP model. Moreover, diborane is also an intriguing molecular system as being a molecule whose structure cannot be rationalized in terms of two-center electron pair bond model, and it has been subjected to many theoretical investigations, both in the gas phase and in solution at the standard condition of pressure.[60–74] At the best of our knowledge, this work reports the first theoretical study of electronic and vibrational properties of the diborane molecule in a dense phase at high pressure.

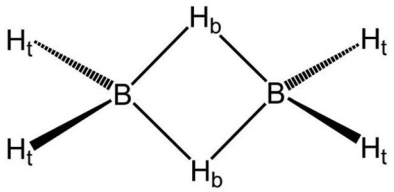

FIG. 1. $B_2H_6(D_{2h})$.

PCM-XP calculations have been performed at the DFT[75–77] level using the M062X[78] hybrid functional and the 6-311++G(d,p) basis set.[79] Atom labels of diborane are shown in Fig. 1. The SES cavity hosting diborane was defined in terms of atomic van der Waals sphere of radii: $R_{vdW}(H) = 1.2$ Å,[81] and $R_{vdW}(B) = 1.92$ Å.[82] Cyclohexane has been used as external nonpolar medium ($\epsilon_0 = 2.0165$, $n_S^0 = 2.581 \times 10^{23}\,\mathrm{cm}^{-3}$, and $R^0_{solv} = 2.815$ Å). To test the dependence of the numerical results with respect to the choice of the repulsive step potential $V_0(N)$, we have performed the calculations for two choices of the amplitude of the repulsive step potential $V_0(3)$ (softer) and $V_0(6)$ (harder), corresponding, respectively, to the use of the $\gamma(3)$ and $\gamma(6)$ amplitudes in Eq. (26).

To make clearer the presentation of the numerical results and of their analysis,[80] this section will be split into three subsections, focused (i) on the pressure as a function of the cavity size, (ii) on the effects of pressure on the equilibrium geometry, and (iii) on the effects of the pressure on the harmonic vibrational frequencies.

A. Cavity size and pressure

As described in Sec. III A, the increase of the pressure, p, is obtained by shrinking the volume V_c of the cavity hosting the diborane molecule. In Fig. 2 we compare the pressure p as a function of the cavity volume V_c, as obtained by using two different choices of the Pauli barrier repulsion potential (see Eq. (26)), namely, the soft repulsive potential $V_0(3)$, and the hard repulsive potential $V_0(6)$. The dependence of the pressure p on the cavity volume V_c is well fitted by a Murnaghan type equation $p = a[(V_c^o/V_c)^b - 1] + c$: with $V_c^o = 83.36$ Å^3, $c = 0.98$ GPa, and $(a, b) = (0.7\,\mathrm{GPa}, 5.813)$ for the barrier step $V_0(3)$, and with $(a, b) = (1.10783\,\mathrm{GPa}, 6.553)$ for the barrier step $V_0(6)$. As expected, the highest repulsive barrier $V_0(6)$ leads to a more rapid increase of the pressure. However, in both cases the values of the parameters

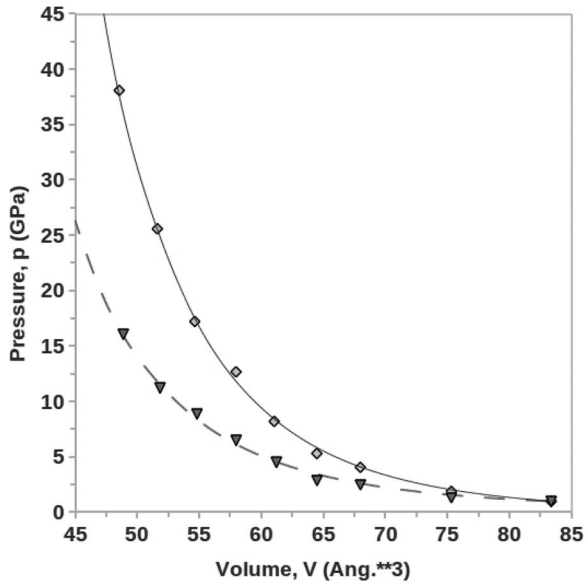

FIG. 2. Pressure, p, (in GPa) as a function of the volume, V_c (in Å^3) of the cavity hosting diborane. The values refer to the PCM/M062X/6-311++G(d,p) level for the Pauli step barriers $V_0(3)$ (▼) and $V_0(6)$ (♦) (see text). The curves correspond to $p = a[(V_C^o/V_C)^b - 1] + c$ with $V_C^o = 83.36$ and $(a, b, c) = (1.1078\,\text{GPa}, 6.553, 0.98\,\text{GPa})$ for the step barrier $V_0(6)$ and $(a, b, c) = (0.710\,\text{GPa}, 5.813, 0.98\,\text{GPa})$ for the step barrier $V_0(3)$.

(a, b) are comparable with the characteristic values of the corresponding parameters of the Murnaghan equation of state for a dense medium at high pressure.[16,83,84]

B. Equilibrium geometries

In Table I, we report the equilibrium geometry of diborane in gas phase and in a dense phase as a function of the pressure. To test the stability of the results with respect to the choice of repulsion barrier step $V_0(N)$, we have performed the geometry optimization using the softer $V_0(3)$ and the harder $V_0(6)$ potentials.

Table I shows that the computed equilibrium geometries in the gas phase are similar to those previously reported in the literature (see Ref. 85 and references therein), and in agreement with the available experimental data.[86]

As reported in Table I, all the boron-hydrogen (terminal), boron-hydrogen (bridge), and boron-boron bond distances show significant pressure effects, with a shortening of the bonds at the increase of the pressure. On the contrary, BHB of the four member ring and the HBH bond angles remain close to their gas phase values. This computational evidence indicates a high rigidity of the shape of the diborane molecules, and is in agreement with recent experimental indications.[21]

Figure 3 presents the plots of the boron-hydrogen bonds distances as a function of the pressure, which exhibit a linear functional dependence. We also note that bond distances computed with the two choices of repulsive potentials $V_0(3)$ (softer) and $V_0(6)$ (harder) exhibit a very similar dependence on the pressure. The finding that a given calculated pressure induces a very similar response of the equilibrium geometry demonstrates the stability of the PCM-XP results with respect to the choice of the repulsive barrier $V_0(N)$.

TABLE I. Equilibrium geometry (see Fig. 1) of diborane as a function of the pressure, p (in GPa): bond distances rBH_t, rBH_b, rBB are in Å and bond angles H_tBH_t, H_bBH_b are in degrees. Results refer to the PCM/DFT/M062X/6-311++G(d,p) level, and using the step barrier potentials $V_0(6)$ (harder) and $V_0(3)$ (softer). Data at 0.0 GPa refer to the gas phase results.

p (GPa)	rBH_t	rBH_b	rBB	H_tBH_t	H_bBH_b
0.0	1.1850	1.3134	1.7564	118.91	96.07
			$V_0(6)$		
0.98	1.1832	1.3131	1.7527	118.92	96.26
1.87	1.1818	1.3122	1.7500	118.93	96.36
4.05	1.1793	1.3105	1.7456	118.94	96.48
5.30	1.1773	1.3087	1.7423	119.02	96.53
8.20	1.1747	1.3053	1.7360	119.02	96.64
12.68	1.1715	1.3027	1.7310	119.02	96.73
17.23	1.1671	1.2982	1.7228	119.05	96.86
25.57	1.1612	1.2926	1.7127	119.10	97.02
38.08	1.1536	1.2851	1.6993	119.15	97.23
			$V_0(3)$		
0.98	1.1832	1.3131	1.7527	118.92	96.26
1.30	1.1822	1.3124	1.7503	118.94	96.35
2.49	1.1806	1.312	1.7470	118.95	96.46
2.86	1.1794	1.3102	1.7447	118.98	96.51
4.34	1.1781	1.3089	1.7418	118.99	96.58
6.48	1.1764	1.3075	1.7385	119.01	96.66
8.87	1.1741	1.3043	1.7319	119.05	96.80
11.21	1.1712	1.3027	1.7284	119.06	96.88
16.06	1.1677	1.2989	1.7209	119.098	97.027

1. The bond distances shortening and the electrostatic forces induced by the pressure

The shortening of the bond distances in diborane may be analyzed in terms of pressure direct effects on the electronic charge distribution.[80]

In Fig. 4, we show the deformations of the electron density of diborane in response to the pressure p, represented as isovalue contours plots of the differential electron density $(\Delta\rho(p) = \rho(p) - \rho(0))$. The phenomenological effect of the pressure is to push the electron distribution away from the peripheral regions corresponding to the hydrogen atoms toward the internuclear bond regions between the terminal and bridge hydrogens and the boron atoms. The cause of this effect is the Pauli repulsive interaction with the external medium, which touches the tails of the electronic charge distribution in the peripheral regions[26,46] of diborane.

The consequences of the reorganization of the electronic distribution $\rho(p)$ may be analyzed by using the force concept based on the Hellmann-Feynman (H-F) electrostatic theorem.[87–91] This force provides a perspective for the electronic origin of the nuclear rearrangement process on a potential-energy surface, connecting the nuclear geometry changes to the electronic distribution changes. The H-F electrostatic forces, and fields, have been used to study the geometries of molecules in the presence of an external electric field, and it can be straightforward generalized to the case of a more general external agent as that we are considering here (i.e., the pressure).

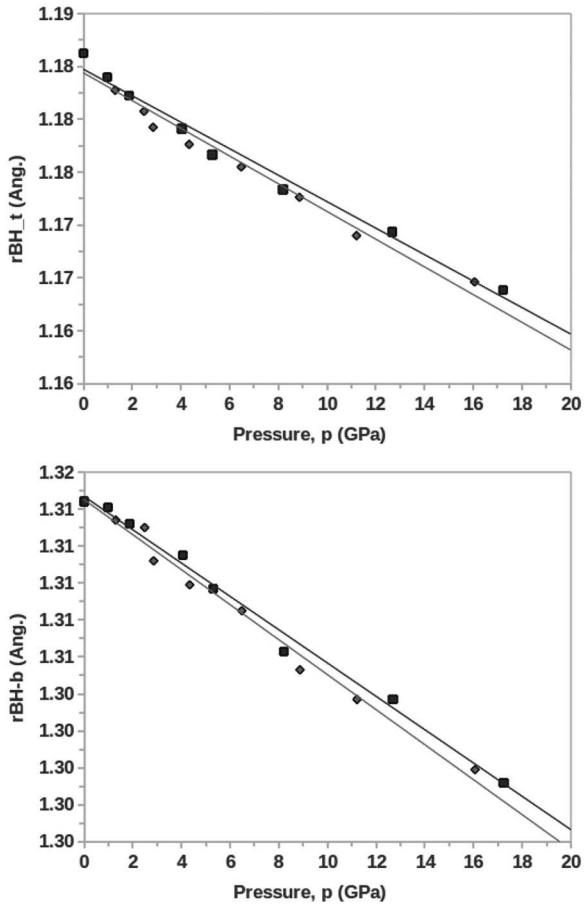

FIG. 3. Boron-hydrogen (BH) equilibrium bond lengths (in Å) of diborane as a function of the pressure (GPa), as computed at the PCM-XP/M062X/6-311++G(d,p) level with the potential barriers $V_0(3)$ (♦) and $V_0(6)$ (■). Boron-hydrogen (bridge) bond lengths, rBH_b, are shown on the bottom and terminal boron-hydrogen, rBH_t, are shown on the top. Regression lines $rBH_t = a + b \times p$ are $(a, b) = (1.1835\,\text{Å}, -0.00105\,\text{Å/GPa})$, with $R^2 = 0.977$, for the $V_0(3)$ potential, and $(a, b) = (1.1838\,\text{Å}, -0.00100\,\text{Å/GPa})$, with $R^2 = 0.983$, for the $V_0(6)$ potential; regression lines $rBH_b = a' + b' \times p$ are $(a, b) = (1.3135\,\text{Å}, -0.00095\,\text{Å/GPa})$, with $R^2 = 0.988$, for the $V_0(3)$ potential, and $(a, b) = (1.3137\,\text{Å}, -0.00090\,\text{Å/GPa})$, with $R^2 = 0.992$, for the $V_0(6)$ potential.

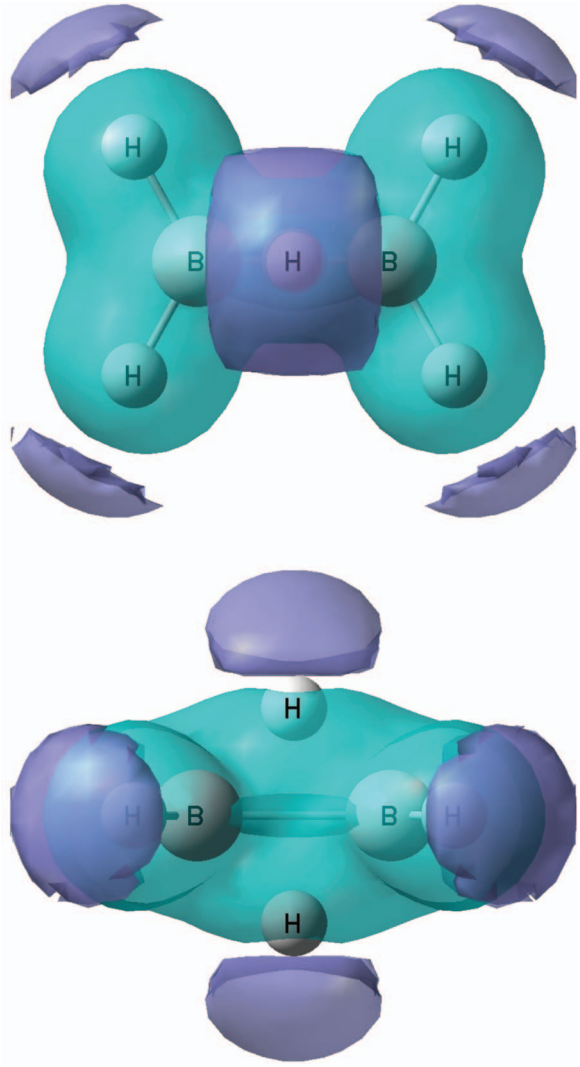

FIG. 4. Isosurface plots of the differential electron density $\delta\rho(p) = \rho(p) - \rho(0)(e^-/a_o^3)$ of B_2H_6 at the PCM-XP/M062X/6-311++G(d,p) level using the potential barriers $V_0(6)$. Isosurfaces refer to the case $p = 0.98$ GPa. Purple isovalues surface denote *depletion* of charges ($\Delta\rho = -8.0 \times 10^{-5} a_o^3$), and green isovalues curves denote *concentration* of charges ($\Delta\rho = 8.0 \times 10^{-5} a_o^3$). Note that, no concentration of electronic charge occurs along the boron-boron axis of the four members ring of diborane.

The *H-F* electrostatic force $\mathbf{F}$ acting on a nucleus A, at $\mathbf{R}_A$, is given by

$$\Delta\mathbf{F}(\mathbf{R}_A) = -Z_A \int \Delta\rho(\mathbf{r}; p) \frac{(\mathbf{r} - \mathbf{R}_A)}{|\mathbf{r} - \mathbf{R}_A|^3} d\mathbf{r},$$

where Z_A is the nuclear charge of A, and $\Delta\rho(\mathbf{r} : p)$ is the differential electronic density induced by the pressure p. We recall that the *H-F* theorem is valid for exact and "stationary" wavefunctions and is approximated with the use of the linear combination of atomic orbitals approximation where the exact forces have to be calculated using the energy gradients.

In Figs. 5 and 6, we show the linear correlation of the *H-F* electrostatic fields at the hydrogen atoms of diborane with the corresponding energy gradient, $G_{e-r}^{\mathbf{R}_H}$, and with the *rBH* bond distances, respectively. These correlations demonstrate that, the pressure effects on the molecular geometry can be interpreted in terms of the electrostatic forces on the nuclei, in analogy with the semiclassical interpretation of several aspects of structural chemistry as chemical substituent effects, and external perturbation effects of various nature.[92–96]

2. The linear dependence on pressure of the bond distances

The potential energy function for the nuclei motion, $G_{e-r}(\mathbf{Q}, p)$, may be formally expressed as a function of the external pressure, p, as

$$G_{e-r}(\mathbf{Q}, p) = G_{e-r}(\mathbf{Q}, 0) + p \sum_i^{TS} \Gamma_i Q_i, \qquad (27)$$

where $G_{e-r}(\mathbf{Q}, 0)$ denotes the potential energy function for the nuclei at $p = 0$ $\mathbf{Q}$, that is, for the isolated molecules, being $\mathbf{Q}$ the corresponding normal vibrational modes, and Γ_i is a

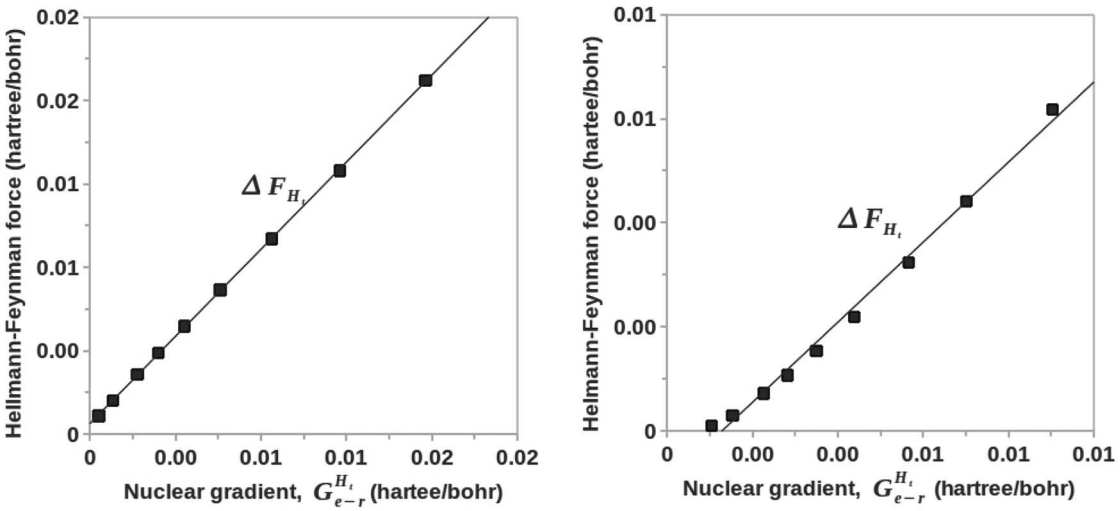

FIG. 5. Correlation between the nuclear gradients G^{H}_{e-r} for the hydrogen atoms and the electric field, $\Delta\mathbf{F}_H$, (in a.u.) induced by the pressure at the same atoms, as computed at the PCM-XP/M062X/6-311++G(d,p) level and using the potential barriers $V_0(6)$. (Left) Terminal boron-hydrogen, $\Delta\mathbf{F}_{H_t}(\|)$ vs $G_{e-r^{H_t}(\|)}$ (R^2 = 1.00). (Right) Bridge boron-hydrogen, $\Delta\mathbf{F}_{H_b}(\|)$ vs $G_{e-r^{H_b}(\|)}$(R^2 = 0.993). $\Delta\mathbf{F}_H(\|)$ and $G_{e-r^{H_b}(\|)}$ denote the component parallel to the pertinent hydrogen-to-boron bond direction of the electric field and of the nuclear gradients, respectively.

pressure coupling parameter defined as

$$\Gamma_i = \left(\frac{\partial^2 G_{e-r}}{\partial p \partial Q_i}\right)_{\mathbf{Q}=0} = \left(\frac{\partial G^{Q_i}_{e-r}}{\partial p}\right)_{\mathbf{Q}=0}. \tag{28}$$

The coupling parameter Γ_i corresponds to a mixed second derivative of the basic PCM-XP energy, which has the physical meaning of a molecular response function describing the response to the pressure of the component of energy gradients along the normal mode coordinates, $G^{Q_i}_{e-r}$. For symmetry reasons, Γ_i is different from zero only for totally symmetric (TS) normal mode coordinates, and therefore the summation of Eq. (27) runs only over these normal coordinates.

In the harmonic (i.e., second order) approximation, the potential energy function for the isolated molecules is given by

$$G_{e-r}(\mathbf{Q}, 0) = G_{e-r}(0, 0) + \frac{1}{2}\sum_i k_i Q_i^2, \tag{29}$$

where $\mathbf{Q} = 0$ denotes the equilibrium geometry in gas phase, and the k_i are the corresponding harmonic force constants.

In the presence of the pressure, the equilibrium geometry corresponds to a stationary point of the potential function $G_{el-rep}(\mathbf{Q}, p)$. With respect to the gas phase geometry, the totally symmetric normal coordinates Q_i experience a shift of their local minima which is determined by the condition:

$$\frac{\partial G_{e-r}(\mathbf{Q}, p)}{\partial Q_i} = p\Gamma_i + k_i Q_i^{eq} = 0, \tag{30}$$

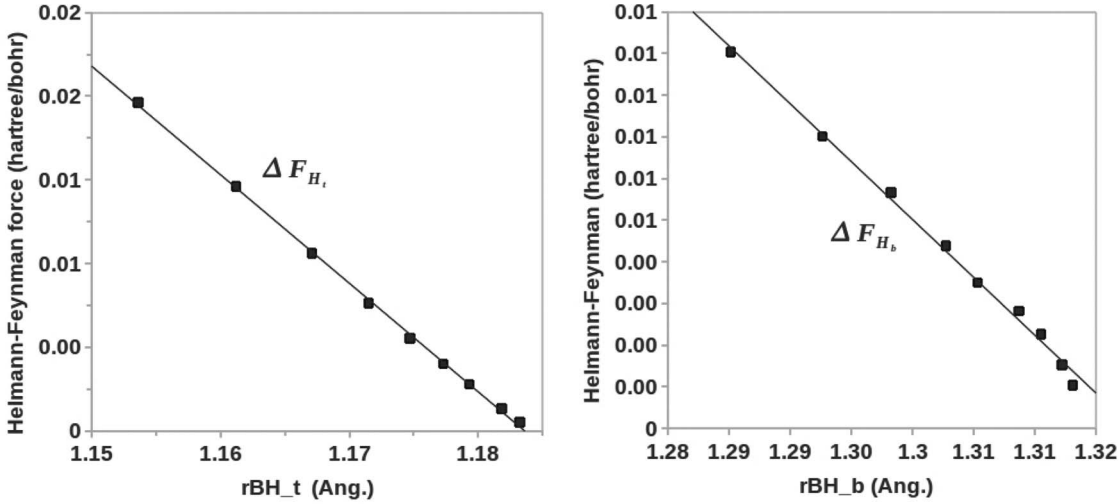

FIG. 6. Correlation between the boron-hydrogen (BH) bond lengths Å of diborane and the electric field, $\Delta\mathbf{F}_H$ (in a.u.) induced by the pressure at the hydrogen atoms, as computed at the PCM-XP/M062X/6-311++G(d,p) level and using the potential barriers $V_0(6)$. (Left) Terminal boron-hydrogen rBH_t vs $\Delta\mathbf{F}_{H_t}(\|)$ (R^2 = 1.00). (Right) Bridge boron-hydrogen rBH_b vs $\Delta\mathbf{F}_{H_b}(\|)$ (R^2 = 0.996). $\Delta\mathbf{F}_H(\|)$ denote the component of the electric field parallel to the pertinent hydrogen-to-boron bond direction.

TABLE II. Pressure coupling constant Γ_i ($E_h\, a_0^{-1}\,\mathrm{GPa}^{-1}$), harmonic force constants in gas phase k_i($E_h\, a_0^{-2}$), ratio Γ_i/ki ($\mathrm{Å\,GPa}^{-1}$), and pressure coefficients dQ_i/dp ($\mathrm{Å\,GPa}^{-1}$)) of diborane (see text). The reported values refer to the PCM/M062X/6-311++G(d,p) level of calculation, for the step barrier potential $V_0(6)$, and regard the totally symmetric normal coordinates Q_1 and Q_2, as approximated by the boron-hydrogen bond distances rBH_t and rBH_b, respectively (see Table III). The pressure coupling Γ_i has been evaluated from linear fitting of the nuclear gradients of diborane $G^{Q_i}_{el-rep}$ as a function of the pressure with the range 0–6 GPa, and at the equilibrium energy in gas phase (see Table S1 of the supplementary material[97]). The pressure coefficients dQ_i^{eq}/dp ($\mathrm{Å\,GPa}^{-1}$)) have been evaluated by linear fitting of the internal coordinates rBH_t and rBH_b, respectively, within the range 0–6 GPa as reported in Table I.

i	Γ_i ($E_h\, a_0^{-1}\,\mathrm{GPa}^{-1}$)	k_i ($E_h a_0^{-2}$)	$-\Gamma_i/k_i$ ($\mathrm{Å\,GPa}^{-1}$)	dQ_i^{eq}/dp ($\mathrm{Å\,GPa}^{-1}$)
1	6.75×10^{-4}	0.2837	-1.26×10^{-3}	-1.39×10^{-3}
2	2.20×10^{-4}	0.1817	-0.58×10^{-3}	-0.89×10^{-3}

with new equilibrium values at

$$Q_i(p)^{eq} = -\frac{\Gamma_i}{k_i} p \qquad i \subseteq \mathrm{TS}. \tag{31}$$

Equation (31) is the key equation in the analysis of the effects of the pressure on the equilibrium geometry of molecular systems: it shows that the changes of the equilibrium geometry of the molecule occur with shifts along the totally symmetric normal coordinate Q_i, the shifts linearly depending on the external pressure p. When a normal coordinate Q_i is dominated by a single set of internal coordinates, Eq. (31) implies a linear correlation between the pertinent internal coordinates and the pressure. This conclusion is in agreement with the linear correlation between the boron-hydrogen bond distances of diborane and the pressure shown in Fig. 2; in fact the stretching along the boron-hydrogen (terminal) and the stretching along the boron-hydrogen (bridge) dominate the totally symmetric normal modes Q_1 and Q_2 of diborane, respectively, as reported in Table III.

Equation (31) can be tested numerically. The pressure coupling parameter Γ_i of Eq. (28) can be estimated by numerical differentiation with respect to the pressure of the nuclear gradients ($G^{Q_i}_{e-r}$),[97] evaluated at the equilibrium geometry in the gas phase, and the force constant k_i can be determined from the calculation of the harmonic frequencies of the isolated molecule (see Table S2 of the supplementary material[97]). Table II shows the numerical values of Γ_i and k_i for the totally symmetric normal coordinates Q_1 and Q_2 of diborane, and compares the ratio Γ_i/k_i with the pressure coefficient dQ_i^{eq}/dp, as computed from the equilibrium geometries of diborane as a function of the pressure (see Table I and Fig. 3).

Finally, we note that by defining the new (i.e., shifted) normal mode coordinates as

$$\tilde{Q}_j = Q_j + \frac{\Gamma_j}{k_j} p, \tag{32}$$

the potential energy function $G_{e-r}(\mathbf{Q}, p)$ can be rewritten as

$$G_{e-r}(\mathbf{Q}, p) = \tilde{G}_{e-r}(0, p) + \frac{1}{2}\sum_i k_i \tilde{Q}_i^2, \tag{33}$$

TABLE III. Symmetry properties and description of the vibrational normal modes of diborane. Diborane has a D_{2h} molecular symmetry and the irreducible representation spanned by the harmonic vibrational modes are: $\Gamma_{D_{2h}}(B_2H_6) = 4A_g + 2B_{1g} + 2B_{2g} + 3B_{2u} + 2B_{1u} + B_{3g} + 3B_{3u}$. Normal modes are classified as ν, stretching; δ, bending; ρ, rocking; ω, wagging; t, twisting; s, symmetric; a, asymmetric.[105]

Mode	Symmetry	Description
1	A_g	ν_s BH_t
2	A_g	Ring stretching (BH_b)
3	A_g	δ_s H_tBH_t
4	A_g	Ring deformation (H_bBH_b)
5	A_u	t BH_2
6	B_{2g}	Ring stretching (BH_b)
7	B_{2g}	ω_s BH_2
8	B_{2u}	ν_a BH_t
9	B_{2u}	ρ BH_t
10	B_{2u}	Ring puckering
11	B_{1g}	ν_a BH_t
12	B_{1g}	ρ_s BH_2
13	B_{1u}	Ring stretching (BH_b)
14	B_{1u}	ω_s BH_2.
15	B_{3g}	t BH_2
16	B_{3u}	ν_a BH_t
17	B_{3u}	Ring stretching (BH_b)
18	B_{3u}	δ_a H_tBH_t

where

$$\tilde{G}_{e-r}(0, p) = G_{e-r}(0, 0) - \frac{1}{2}\sum_i \frac{\Gamma_i^2}{k_i} p^2. \tag{34}$$

Equation (34) shows that the harmonic force constants are unaffected by the pressure. To recover the effect of the pressure on the harmonic force constant we must go beyond the double harmonic approximation of Eqs. (27) and (29), as will be discussed in Sec. IV C.

C. Harmonic vibrational frequencies

Table III shows the normal vibrational modes of the diborane molecule classified according to the irreducible representations of the D_{2h} symmetry point group, and described in terms of the dominant internal symmetry coordinates.

Table IV reports the computed harmonic vibrational frequencies of diborane in the gas phase and as a function of the pressure. As described in Sec. III, the harmonic vibrational frequencies have been computed for each pressure value at the corresponding equilibrium geometry. For the sake of simplicity, the results reported in Table IV only refer to the hardest repulsive potential $V_0(6)$. The corresponding results obtained using the softest repulsive potential $V_0(3)$ are reported in Table S3 of the supplementary material.[97]

The computed harmonic frequencies of diborane in the gas phase of Table IV are in close agreement with the previous calculations reported in the literature[85,98–104] and with the experiments.[105]

All the harmonic vibrational frequencies of diborane increase as the pressure increases (Table IV). The dependence of the harmonic vibrational frequencies on the pressure is

TABLE IV. Harmonic vibrational frequencies (in cm^{-1}) of diborane as a function of the pressure, p (GPa). Results refer to the PCM/DFT/M06/6-311++G(d,p) level for the barrier potential $V_0(6)$. Data at 0.0 GPa refer to the gas phase. No scaling factors have been applied to the harmonic vibrational frequencies.

		p (GPa)								
Mode	Symmetry	0.0	1.0	1.9	4.1	5.3	12.7	17.2	25.6	38.1
1	A_g	2667	2681	2692	2710	2725	2767	2800	2846	2911
2	A_g	2175	2180	2184	2192	2201	2233	2260	2294	2344
3	A_g	1202	1207	1211	1218	1225	1245	1260	1280	1308
4	A_g	815	821	825	833	840	861	878	899	927
5	A_u	858	866	870	879	884	910	929	952	987
6	B_{2g}	1874	1882	1886	1894	1901	1929	1951	1983	2025
7	B_{2g}	893	901	905	911	916	935	950	967	992
8	B_{2u}	2756	2770	2781	2801	2817	2863	2898	2947	3015
9	B_{2u}	950	955	958	963	967	980	990	1005	1026
10	B_{2u}	330	337	341	348	356	381	400	426	462
11	B_{1g}	2743	2758	2769	2790	2806	2852	2888	2938	3006
12	B_{1g}	928	930	933	937	942	957	969	984	1006
13	B_{1u}	2011	2015	2023	2035	2047	2086	2117	2156	2213
14	B_{1u}	999	1001	1004	1011	1014	1033	1048	1065	1091
15	B_{3g}	1049	1054	1057	1062	1066	1080	1092	1108	1131
16	B_{3u}	2652	2666	2677	2696	2711	2754	2788	2835	2901
17	B_{3u}	1715	1704	1705	1709	1715	1737	1758	1786	1826
18	B_{3u}	1190	1193	1196	1202	1208	1227	1241	1261	1288

described satisfactorily by a linear relationship, as shown in Fig. 7 for the totally symmetric normal modes of the diborane molecule.

In the following, we will present an interpretation of linear dependence of the harmonic vibrational frequencies on the pressure, in the light of a theoretical scheme analogous to that already introduced in Sec. IV B for the analysis of pressure effects on the equilibrium geometry. The subsection will be closed by a comparison with the available experimental data of the pressure effects on the vibrational frequencies of diborane.

1. The linear dependence of the harmonic vibrational frequencies

Let us consider an extension up to the third order of above introduced formalism to analyze the effect of the pressure on the equilibrium geometry. The potential function for the nuclei motion is written as

$$G_{e-r}(\mathbf{Q}, p) = G_{e-r}(\mathbf{Q}, 0) + p \sum_i \Gamma_i Q_i + p \sum_i \Gamma_{ii} Q_i^2 + \cdots, \tag{35}$$

where we have introduced an additional contribution of first order in the pressure p and of second order in the vibrational normal modes, with the second-order pressure coupling parameter Γ_{ii} defined as

$$\Gamma_{ii} = \left(\frac{\partial^3 G_{e-r}}{\partial p \partial^2 Q_i}\right)_{\mathbf{Q}=0} = \left(\frac{\partial k_i}{\partial p}\right)_{\mathbf{Q}=0}. \tag{36}$$

The second-order coupling parameter Γ_{ii} corresponds to a mixed third derivative of the basic PCM-XP energy representing the response to the pressure of the force constant k_i of the ith normal mode. Γ_{ii} may be different from zero for any vibrational normal mode. In the expansion (35) we have neglected third order terms $p\Gamma_{ij}Q_iQ_j$ that describe the effects of the pressure on the mixing of normal modes.

The third-order expansion for the potential energy function of the isolated molecule may be written as[106]

$$G_{e-r}(\mathbf{Q}, 0) = G_{e-r}(0, 0) + \frac{1}{2}\sum_i k_i Q_i^2 + \frac{1}{2}\sum_i^{\mathrm{NTS}}\sum_j^{\mathrm{TS}} g_{iij} Q_i^2 Q_j + \frac{1}{2}\sum_i^{\mathrm{TS}}\sum_{j\neq i}^{\mathrm{TS}} g_{iij} Q_i^2 Q_j + \frac{1}{6}\sum_i^{\mathrm{TS}} g_{iii} Q_i^3, \tag{37}$$

with NTS and TS denoting summations, respectively, over the nontotally symmetric, and over the totally symmetric normal modes; g_{iij} denotes a cubic anharmonic coupling between the generic normal mode i and a totally symmetric normal mode j ($g_{iij} = \partial^3 G_{e-r}/\partial^2 Q_i \partial Q_j$). In the expansion (37) we have neglected once again third order terms $g_{ijk}Q_iQ_jQ_k$ that describe effects of the pressure on the mixing of normal modes.

Introducing the shifted normal coordinates $\tilde{Q}_i = Q_i + \Gamma_i/k_i p$, the potential energy function (35) can be rewritten as

$$G_{e-r}(\tilde{\mathbf{Q}}, p) = \tilde{G}_{e-r}(0, p) + \frac{1}{2}\sum_i \tilde{k}_i(p)\tilde{Q}_i^2, \tag{38}$$

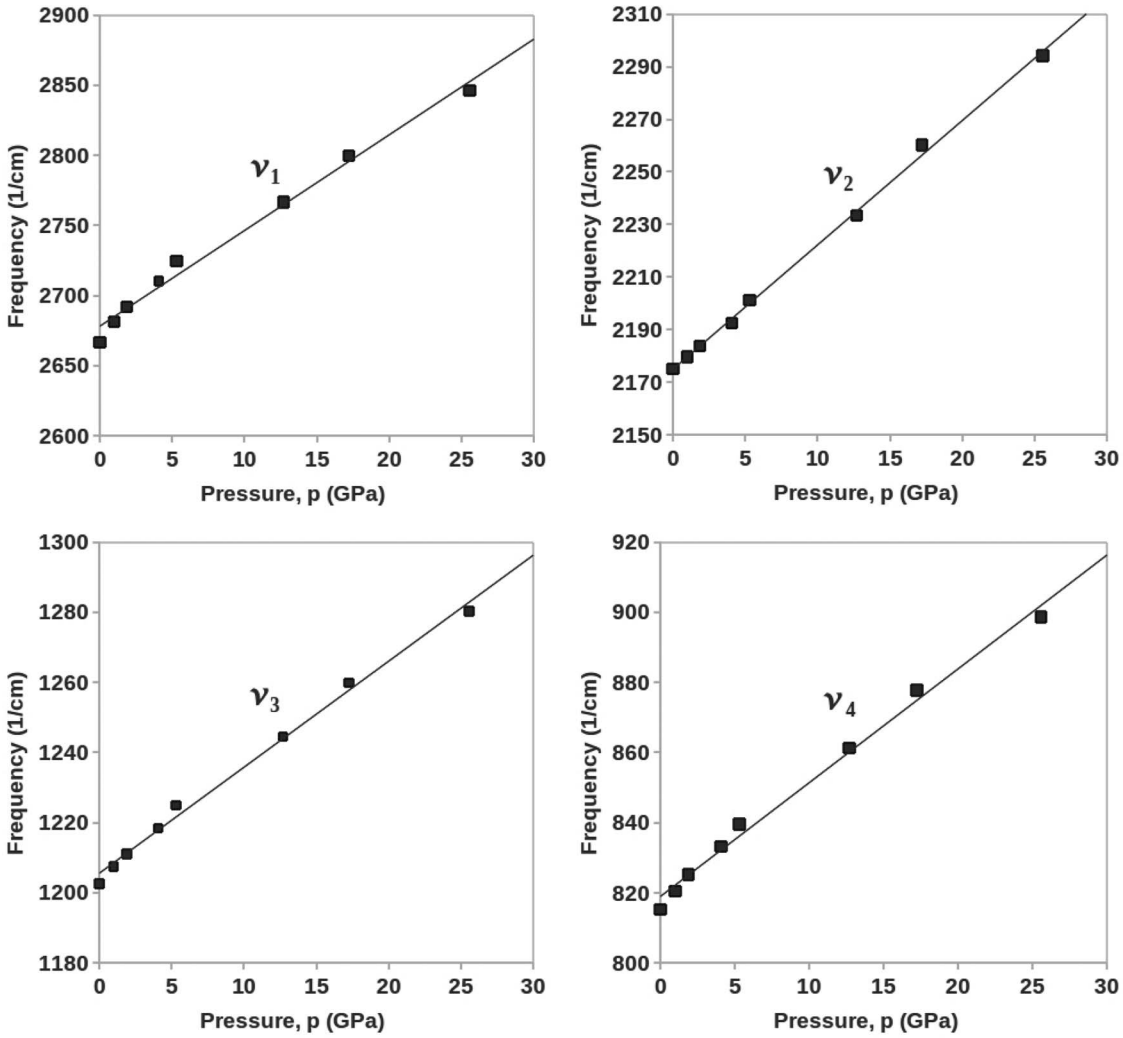

FIG. 7. Correlations between the harmonic vibrational frequencies and the pressure for the totally symmetric modes of diborane: ν_1 ($R^2 = 0.988$), ν_2 ($R^2 = 0.998$), ν_3 ($R^2 = 0.994$), ν_4 ($R^2 = 0.992$). The values refer to the PCM-XP/M062X/6-311++G(d,p) level using the potential barriers $V_0(6)$.

where $\tilde{G}_{e-r}(0, p)$ is given by

$$\tilde{G}_{e-r}(0,P) = G_{e-r}(0,0) - p^2\frac{1}{2}\sum_i^{TS}\left(\frac{\Gamma_i}{k_i}\right)^2 - p^3\frac{1}{2}\sum_{j\neq k}^{TS} g_{jjk}\left(\frac{\Gamma_j}{k_j}\right)^2\frac{\Gamma_k}{k_k} + p^3\frac{1}{6}\sum_j^{TS} g_{jjj}\left(\frac{\Gamma_j}{k_j}\right)^3 + p^3\frac{1}{2}\sum_i^{TS}\Gamma_{ii}\left(\frac{\Gamma_i}{k_i}\right)^2 \tag{39}$$

and $\tilde{k}_i(p)$ is the harmonic force constant at the pressure p:

$$\tilde{k}_i(p) = k_i + p\left(\Gamma_{ii} - \sum_j^{TS}\frac{g_{iij}\Gamma_j}{k_j}\right). \tag{40}$$

Equation (40) is central in the analysis of the pressure effects, as it shows that *the harmonic force constants are linear functions of the pressure*, with coefficient:

$$\frac{\tilde{k}_i}{dp} \equiv \left(\frac{\partial^3 G_{e-r}}{\partial p \partial^2 Q_i}\right)_{\mathbf{Q}^{eq}} = \left(\Gamma_{ii} - \sum_j^{TS}\frac{g_{ij}\Gamma_j}{k_j}\right). \tag{41}$$

Equation (40) is also the starting point for the analysis of pressure effects on the vibrational force constant in terms of two contributions: the "curvature" and the "relaxation" contributions.[80,107,108] In fact, the pressure coefficients of Eq. (40), $d\tilde{k}_i/dp$ may be rewritten as

$$\frac{d\tilde{k}_i}{dp} = \left.\frac{dk_i}{dp}\right|_{cur} + \left.\frac{dk_i}{dp}\right|_{rel}, \tag{42}$$

with

$$\left.\frac{dk_i}{dp}\right|_{cur} = \Gamma_{ii}, \tag{43}$$

and

$$\left.\frac{dk_i}{dp}\right|_{rel} = -\sum_j^{TS}\frac{g_{ij}\Gamma_j}{k_j}. \tag{44}$$

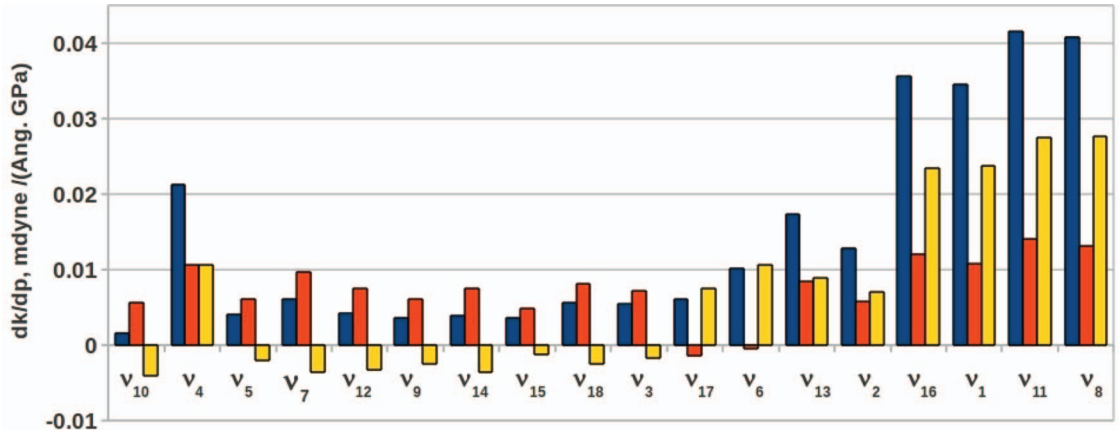

FIG. 8. Pressure coefficients of the force constants, (dk_i/dp) (in blue) and their components *curvature*, $(dk_i/dp)_{cur}$ (in red) and *relaxation*, $(dk_i/dp)_{rel}$ (in yellow), for the 18 normal modes of diborane. The data (in mdyn Å^{-1} GPa^{-1}) refer to the PCM-XP/M062X/6-311++G(d,p) level using the potential barriers $V_0(6)$.

The meaning of the two contributions to the pressure coefficient $d\tilde{k}_i/dp$ is easy to understand. The term $dk_i/dp|_{cur}$ describes the effects of the pressure on the *curvature* of the PES at the fixed equilibrium geometry in gas phase, and it corresponds to the response function Γ_{ii} defined in Eq. (36); while the term $dk_i/dp|_{rel}$ of Eq. (44) describes the effects of the pressure due to the *relaxation* of equilibrium geometry along the totally symmetric normal modes $\{j\}$, and it depends on the cubic anharmonic coupling constants g_{iij} between modes i, j.

Equations (40)–(44) can be evaluated numerically. The pressure coefficients $d\tilde{k}_i/dp$ can be determined from the linear regression between the force constant $\tilde{k}_i(p)$, computed at the pressure p and at the corresponding equilibrium geometry, and the pressure p itself (see Table S4 of the supplementary material[97]). The pressure coefficients $dk_i/dp|_{cur}$ may be computed in the similar way by considering the force constant $k_i(p)$ computed at the pressure p and at the fixed equilibrium geometry of diborane in the gas phase (see Table S5 of the supplementary material[97]). Finally, the pressure coefficients $dk_i/dp|_{rel}$ may be determined as a difference from Eq. (42). Figure 8 shows the numerical results of curvature ($dk_i/dp|_{cur}$ in red) and relaxation ($dk_i/dp|_{rel}$ in yellow) pressure coefficients for the 18 normal modes of diborane (the normal modes are ordered from left to the right of Fig. 8 with increasing of the harmonic vibrational frequency). The curvature effect of the pressure on the harmonic force constant (i.e., $dk_i/dp|_{cur}$) of diborane is positive for almost all the normal modes, while the relaxation effect (i.e., $dk_i/dp|_{rel}$) may present both signs. A positive sign of $dk_i/dp|_{rel}$ indicates that the relaxation of equilibrium geometry determines an increase of the harmonic force constant k_i, while a negative sign of $dk_i/dp|_{rel}$ denotes the opposite case, in which the relaxation of equilibrium geometry determines a decrease of the force constant k_i.

As a further example of the potentialities of the present analysis, we show in Fig. 9 the correlation between the relaxation pressure coefficient $dk_i/dp|_{rel}$ of the 18 normal modes of diborane with the corresponding leading anharmonic coupling contribution $g_{iij}\Gamma_j/k_j$ (see Table S6 of the supplementary material for the values of g_{iij}[97]). The good linear correlation ($R^2 = 0.975$) is in agreement with the definition of $dk_i/dp|_{rel}$ in Eq. (44).

The linear relationship (40) between the force constant of the normal modes and the pressure implies a linear relationship between the vibrational harmonic frequencies and the pressure:

$$\tilde{\nu}_i = \nu_i + p\left[\frac{1}{2}\left(\frac{\nu_i}{k_i}\right)\frac{d\tilde{k}_i}{dp}\right], \tag{45}$$

where ν_i is the harmonic frequency of the unperturbed mode, and $d\tilde{k}_i/dp$ is the pressure coefficient of the force constant. The linear correlation between harmonic vibrational frequencies and the pressure, as expressed by Eq. (45), is in agreement with the numerical evidence reported in Table IV and in Fig. 6.[109]

A further useful linear relationship, between the vibrational frequencies $\tilde{\nu}_i$ and the shifts of the totally symmetric normal modes Q_i^{eq}, can be derived combining Eqs. (31) and (45):

$$\tilde{\nu}_i = \nu_i - \frac{1}{2}\left(\frac{\nu_i}{\Gamma_i}\right)\frac{d\tilde{k}_i}{dp}Q_i^{eq}. \tag{46}$$

Equation (46) may be considered as an expression of the Badger rule[49] connecting the force constants and the equilibrium

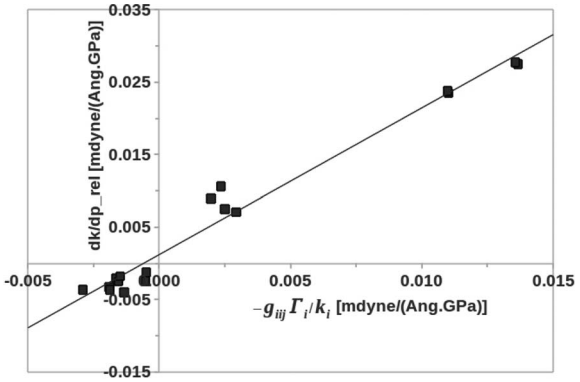

FIG. 9. Correlation ($R^2 = 0.975$) between the curvature pressure coefficient $(dk_i/dp)_{cur}$ and the corresponding leading term $g_{iij}\Gamma_j/k_j$ of Eq. (44). The data (in mdyn Å^{-1} GPa^{-1}) refer to selected normal modes of diborane, as computed at the PCM-XP/M062X/6-311++G(d,p) level using the potential barriers $V_0(6)$. See Table S5 of the supplementary materials for the values of the cubic force constant g_{iij} for diborane in gas phase.[97]

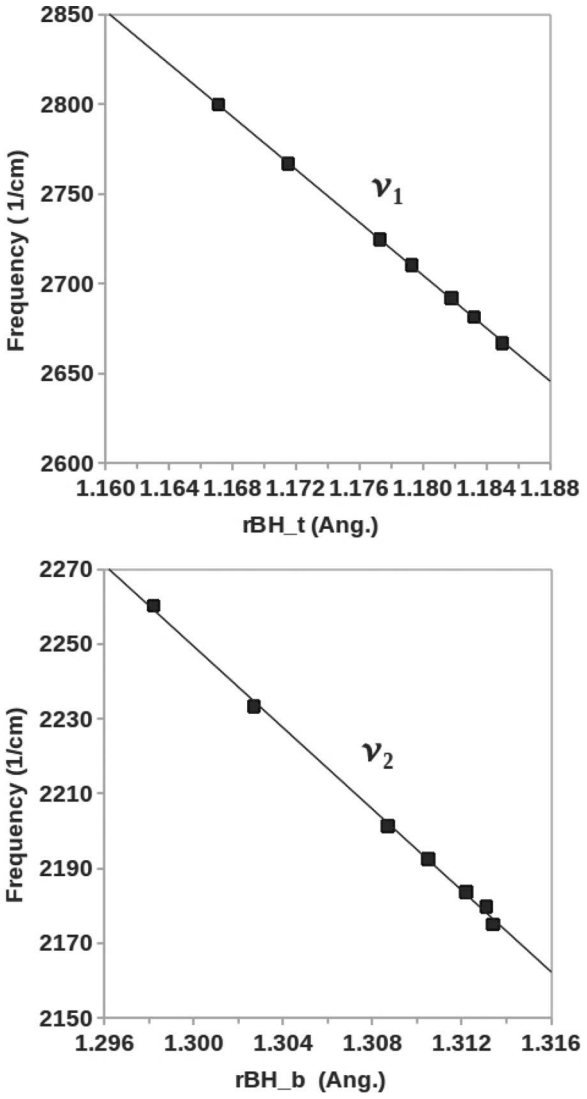

FIG. 10. Correlation between the harmonic vibrational frequencies (cm^{-1}) and the boron-hydrogen bond lengths (Å). (Top) The totally symmetric normal modes ν_1 vs the terminal boron-hydrogen bond length ($R^2 = 1.00$). (Bottom) The totally symmetric normal modes ν_2 vs the terminal boron-hydrogen bond length ($R^2 = 1.00$). Values refer to the PCM-XP/M062X/6-311++G(d,p) level using the potential barriers $V_0(6)$.

geometry of molecular systems. When a normal coordinate Q_i is dominated by a single set of internal coordinate, Eq. (46) implies a linear correlation between the vibrational frequencies and the pertinent internal coordinates. Figure 10 shows the linear correlation between the harmonic vibrational frequencies of the totally symmetric normal modes ν_1, ν_2 and the boron-hydrogen bond lengths rBH_t and rBH_b of diborane, respectively.

2. Comparison with the experimental data

Finally, we compare the computed harmonic frequencies of diborane as a function of the pressure with the available experimental data. High pressure Raman and IR spectroscopies studies of diborane in its condensed phases have been recently reported.[20,21] In these studies, the pressure dependences of the several internal modes of diborane have been used to identify pressure dependent structure transformations of the phases. Several structural transformations have been identified starting from a liquid-phase I transition around 4 GPa. In Table V, we compare the pressure dependent data of the liquid phase (0–4 GPa) with the computed pressure coefficients $(d\nu/dp)_{th}$ of the harmonic vibrational frequencies. The comparison shows that the results of the PCM-XP model give a reasonable description of the experimental pressure effect on the vibrational frequencies of diborane.

TABLE V. Comparison between the computed pressure coefficients $(d\nu/dp)_{th}$ of the harmonic vibrational frequencies of diborane and the available experimental data $(d\nu/dp)_{exp}$ from Refs. 20 and 21. The computed pressure coefficients refer to the range of pressure 0–6 GPa, and at the PCM/DFT/M062X/6-311++G(d,p) level using the step barriers $V_0(6)$ and $V_0(3)$. The experimental pressure coefficients refer to the diborane in liquid phase (0–4 GPa). All the values are in cm^{-1}/GPa.

		$(d\nu/dp)_{th}$		
Mode	Symmetry	$V_0(6)$	$V_0(3)$	$(d\nu/dp)_{exp}$
1	A_g	10.4	9.6	12.9
2	A_g	4.8	4.6	7.9
3	A_g	4.1	4.0	2.6
4	A_g	4.4	4.7	8.6
5	A_u	4.6	5.0	...
6	B_{2g}	4.8	4.8	7.9
7	B_{2g}	4.0	3.9	...
8	B_{2u}	11.0	10.2	...
9	B_{2u}	3.0	2.7	...
10	B_{2u}	4.6	4.8	...
11	B_{1g}	11.5	10.5	12.9
12	B_{1g}	2.6	2.6	...
13	B_{1u}	6.7	7.0	...
14	B_{1u}	2.9	2.9	~3
15	B_{3g}	2.9	2.6	−5.7
16	B_{3u}	10.7	9.8	~7
17	B_{3u}	2.5	2.3	~3
18	B_{3u}	3.3	3.2	...

V. SUMMARY

We have presented a new quantum chemical method for the calculation of the equilibrium geometry and the harmonic vibrational frequencies of molecular systems in dense medium at high pressures (of the order of GPa). The new computational method, named PCM-XP, is based on the polarizable continuum model, amply used for the study of the solvent effects at standard condition of pressure, and it is accompanied by a new theory for the analysis and the interpretation of the mechanisms underpinning the effects of pressure on the molecular geometries and the harmonic vibrational frequencies. The PCM-XP has been applied at the density functional theory level to diborane as a molecular system under high pressure. The computed harmonic vibrational frequencies as a function of the pressure have shown a satisfactory agreement with the corresponding experimental results, and the parallel application of the method of analysis has shown that the effects of the pressure on the equilibrium geometry can be interpreted in terms of direct effects on the electronic charge

distribution of the molecular solutes, and that the effects on the harmonic vibrational frequencies can be described in terms of two physically distinct effects of the pressure (*curvature* and *relaxation*) on the potential energy for the motion of the nuclei. These results indicate, in our opinion, the potentialities of PCM-XP method to open new perspectives for the extension of quantum chemistry to the study of pressure effects on the vibrational properties of molecular systems.

ACKNOWLEDGMENTS

This paper is dedicate to the memory of the recently passed away Professor R.W.F. Bader, with which the corresponding author R.C. has shared a common interest toward the exploration of the pressure effects within the framework of modern quantum chemistry. R.C. also thanks Professor B. Kirtman for an accurate and critical reading of the original manuscript. The financial support of the Gaussian Inc. is acknowledged.

APPENDIX: PAULI REPULSION BARRIER

The height V_0 of the Pauli repulsion barrier of Eq. (26) is determined by the parameter $\gamma_N(f)$, depending on the cavity scaling factor f. The functional dependence of $\gamma_N(f)$ can be estimated from the pV experimental data characterizing the external medium, as described in the following.

Using a heuristic approach, we introduce a functional dependence for $\gamma(f)$ with the following form:

$$\gamma(f) = (f_0/f)^N,$$

where f_0 and f are, respectively, the reference and the actual cavity scaling factors. The estimation of the exponential parameter N is performed by computing the pressure p from Eq. (12) as a function of the volume V_c of the cavity, and fitting the computed pV data in terms of an equation of state of the Murnaghan type[16,83,84]

$$p = a\left[\left(V_c^o/V_c\right)^b - 1\right] + c,$$

where V_c^o and V_c are, respectively, the cavity volume at the standard condition of pressure and at the pressure p, and a, b, c are empirical parameters. The best range values of parameters N can be estimated on the basis of the comparison with the experimental pV Murnaghan equation of state for the external medium $p = a[(V_o/V)^b - 1]$, where V^o and V are molar volumes of the medium (see Table VI). Numerical tests show that the range $N = 3$–6 is a reasonable choice for the exponential of functional form of the parameter $\gamma(N)$.

As a historical note, we recall that this type of comparison with the pV experimental data has been first suggested by LeSar and Herschbach in a parenthetical observation of their seminal papers on a rigid spheroidal box model for the description of the electronic and vibrational properties of the hydrogen molecule at high pressure.[49]

TABLE VI. Murnaghan equations of state $p = a[(V_o/V)^b - 1]$ for benzene,[16] cyclohexane,[83] and argon.[84]

Compound	a (GPa)	b
Benzene	1.0	6.5
Cyclohexane	4.8	5.0
Argon	2.0	3.9

[1] R. Cammi, V. Verdolino, B. Mennucci, and J. Tomasi, Chem. Phys. **344**, 135 (2008).
[2] S. Miertuš, E. Scrocco, and J. Tomasi, Chem. Phys. **55**, 117 (1981).
[3] R. Cammi and J. Tomasi, J. Comp. Chem. **16**, 1449 (1995).
[4] E. Cancès, B. Mennucci, and J. Tomasi, J. Chem. Phys. **107**, 3032 (1997).
[5] J. Tomasi, R. Cammi, B. Mennucci, C. Cappelli, and S. Corni, Phys. Chem. Chem. Phys. **4**, 5697 (2002).
[6] J. Tomasi, B. Mennucci, and R. Cammi, Chem. Rev. **105**, 2999 (2005).
[7] R. J. Hemsley, Ann. Rev. Phys. Chem. **51**, 763 (2000).
[8] P. F. McMillan, Nat. Mater. **1**, 18 (2002).
[9] H. K. Mao and D. R. Herschbach, in *Chemistry Under Extreme Conditions*, edited by R. Manaa (Elsevier, Amsterdam, 2005), p. 189.
[10] V. Schettino and R. Bini, Chem. Soc. Rev. **36**, 869 (2007).
[11] R. D. Etters and A. Helmy, Phys. Rev. B **27**, 6439 (1983).
[12] C. J. Sandroff, H. E. King, Jr., and D. R. Herschbach, J. Phys. Chem. **88**, 5647 (1984).
[13] M. R. Zakin and D. R. Herschbach, J. Chem. Phys. **83**, 6540 (1985).
[14] M. R. Zakin and D. R. Herschbach, J. Chem. Phys. **85**, 2376 (1985).
[15] M. M. Thiéry and J. M. Lager, J. Chem. Phys. **89**, 4255 (1988).
[16] M. M. Thiéry, J. M. Besson, and J. L. Bribes, J. Chem. Phys. **96**, 2633 (1992).
[17] L. Moroni, M. Ceppatelli, C. Gellini, P. R. Salvi, and R. Bini, Phys. Chem. Chem. Phys. **4**, 5761 (2002).
[18] Y. Song, R. J. Hemlet, Z. Liu, M. Somayazulu, H. Mao, and D. R. Herschbach, J. Chem. Phys. **119**, 2232 (2003).
[19] V. Schettino, R. Bini, G. Cardini, M. Ceppatelli, M. Citroni, and M. Pagliai, J. Mol. Struct. **924–926**, 2 (2009).
[20] C. Murli and Y. Song, J. Phys Chem. B **113**, 13509 (2009).
[21] Y. Song, C. Murli, and Z. Liu, J. Chem. Phys. **131**, 174506 (2009).
[22] The pressure is not amenable to a mechanical perturbation, i.e., to a perturbation that represents the action of an external field and that can be completely described by adding into the Hamiltonian the interaction energy of the system with the external field. The action of the pressure is connected to the work done on the system to produce a variation of its volume, and, therefore, the pressure is not related to any real external field.[23]
[23] D. N. Zubarev, *NonEquilibrium Statistical Thermodynamics* (Plenum, New York, 1974).
[24] V. Schettino and R. Bini, Phys. Chem. Chem. Phys. **5**, 1951 (2003).
[25] V. Schettino, R. Bini, M. Ceppatelli, L. Ciabini, and M. Citroni, "Chemical reactions at very high pressure," in *Advances in Chemical Physics*, edited by S. A. Rice (Wiley, New York, 2005), Vol. 131.
[26] W. Grochala, R. Hoffmann, J. Feng, and N. W. Ashcroft, Angew., Chem., Int. Ed. **46**, 3620 (2007).
[27] V. Labet, R. Hoffmann, and N. W. Ashcroft, J. Chem. Phys. **136**, 074502 (2012).
[28] C. Amovilli and B. Mennucci, J. Phys. Chem. B **101**, 1051 (1997).
[29] F. J. Olivares del Valle and J. Tomasi, Chem. Phys. **114**, 231 (1987); R. Cammi, C. Cappelli, S. Corni, and J. Tomasi, J. Phys. Chem. A **104**, 9874 (2000); S. Corni, C. Cappelli, R. Cammi, and J. Tomasi, *ibid.* **105**, 8310 (2001); C. Cappelli, S. Corni, and J. Tomasi, J. Chem. Phys. **115**, 5531 (2001); C. Cappelli, S. Corni, B. Mennucci, R. Cammi, and J. Tomasi, J. Phys. Chem. A **106**, 12331 (2002); C. Cappelli, "Continuum solvation approach to vibrational properties," in *Continuum Solvation Models in Chemical Physics*, edited by B. Mennucci and R. Cammi (Wiley, New York, 2007), pp. 167–179.
[30] The nonequilibrium solvation accounts for the dynamical aspects of the solvent polarization. This polarization can be partitioned into different contributions each related to the various degrees of freedom of the solvent molecules (i.e., translations, rotations, vibrations, electronic motions), which span different orders of magnitude in the corresponding relaxation times. In the common practice, such contributions are collected into two terms only: one term accounts for all the degrees of freedom which involve motions slower than those involved in the physical phenomena under examination, the other includes the faster contributions. As a further assumption, only the latter can be instantaneously equilibrated with the momentary charge distribution whereas the former cannot readjust. In the case of the study of vibrations of solvated molecules, the slow term contains the contributions arising from the translational and rotational

motions of solvent molecules. The assumption that the geometry of the molecular cavity does not follow the solute vibrational motion is then justified by the consideration that the geometry of the cavity is determined by the space non-accessible to the translational and rotational degrees of freedom of the solvent molecules.

[31] R. Cammi and J. Tomasi, J. Chem. Phys. **101**, 3888 (1994); B. Mennucci, R. Cammi, and J. Tomasi, *ibid.* **110**, 6858 (1999); M. Cossi, G. Scalmani, N. Rega, and V. Barone, *ibid.* **117**, 43 (2002); G. Scalmani and M. J. Frisch, *ibid.* **132**, 114110 (2009).

[32] B. Mennucci, R. Cammi, and J. Tomasi, Int. J. Quantum Chem. **75**, 767 (1999).

[33] R. Cammi, L. Frediani, B. Mennucci, J. Tomasi, K. Ruud, and K. V. Mikkelsen, J. Chem. Phys. **119**, 5818 (2002).

[34] Note that the integration variable $\mathbf{r}$ of the kernel $\hat{V}_r(\mathbf{r})$ of operator $\hat{V}_r$ it is not a dynamical variable of the molecular system. The operative definition of the integral kernel $\hat{V}_r(\mathbf{r})$ is given by

$$\langle \Psi \hat{V}_r \Psi \rangle = \int \langle \Psi \hat{V}_r(\mathbf{r}) \Psi \rangle d\mathbf{r}.$$

[35] The PCM-IEF definition of the apparent charges is exact provided that all of the molecular charge distribution is entirely enclosed within the molecular cavity. However, it has been shown both theoretically and numerically that for IEF-PCM the error made due to the escaped charge distribution is negligible in the practical calculations, where the total amount of the escaped charge is lower than a few percent of that of the total electronic charge.[36–39] Also in the numerical applications of the PCM-XP model we have verified that this condition has been satisfied for all the cavity sizes corresponding to the considered range of cavity scaling factor $f = 1.2$–0.95 (see Table S1 of the supplementary material[97]).

[36] D. M. Chipman, J. Chem. Phys. **112**, 5558 (2000).

[37] E. Cancès and B. Mennucci, J. Chem. Phys. **115**, 6130 (2001).

[38] E. Cancès, *Continuum Solvation Models in Chemical Physics*, edited by B. Mennucci and R. Cammi (Wiley, New York, 2007).

[39] D. M. Chipman, J. Chem. Phys. **116**, 10129 (2002).

[40] Here, we do not consider the amount of work for the creation of the cavity within the medium at the given condition of pressure, as it is not involved in the calculation of the harmonic vibrational frequencies of the solute within a cavity with a fixed geometry. The free-energy of cavitation must be considered in the case of the exploration of larger portions of the potential energy surface, and its evaluation at high-pressure regimes will be considered in a forthcoming paper.

[41] J. D. Jackson, *Classical Electrodynamics* (Wiley, New York, 1999).

[42] W. Byers Brown, J. Chem. Phys. **28**, 522 (1958).

[43] G. Marc and W. G. McMillan, Adv. Chem. Phys. **58**, 209 (1985).

[44] We recall that there is another approach to the quantum definition of pressure. This approach has been proposed by R. F. W. Bader, and it is rooted on the definition of atoms in molecules as open systems, a system bounded by a surface of zero flux in the gradient vector field of the electron density.[45] The pressure acting on an open system is determined as the quantum force exerted per unit area of the surface enclosing the system. See for this point the recent review[46] and the references therein.

[45] R. F. W. Bader, *Atoms in Molecules: A Quantum Theory* (Oxford University Press, UK, 1990).

[46] R. F. W. Bader, "Confined atoms treated as open quantum systems," in *Advances in Quantum Chemistry* (Elsevier, Amsterdam, 2009), Vol. 57.

[47] C. A. ten Seldam and S. R. de Groot, Physica **18**, 891 (1952).

[48] E. V. Ludeña, J. Chem. Phys. **69**, 1770 (1978).

[49] R. LeSar and D. R. Herschbach, J. Phys. Chem. **85**, 2798 (1981).

[50] R. LeSar and D. R. Herschbach, J. Phys. Chem. **87**, 5202 (1983).

[51] J. Gorecki and W. Byers Brown, J. Chem. Phys. **89**, 2138 (1988).

[52] J. P. Connerade and R. Smaoune, J. Phys. B **33**, 3467 (2000).

[53] K. D. Sen, B. Mayer, P. C. Schmidt, J. Garza, R. Vragas, and A. Vela, Int. J. Quantum Chem. **90**, 491 (2002).

[54] S. A. Cruz and J. Soullard, Chem. Phys. Lett. **391**, 138 (2004).

[55] R. Cammi, B. Mennucci, and J. Tomasi, J. Phys. Chem. A **102**, 870 (1998).

[56] As pointed out by one of the reviewers, the uniform scaling of the entire system (solute-external medium) implies the approximation to assume the same compressibilities for the solute and for the external medium.

[57] C. J. F Böttcher, *Theory of Electric Polarization* (Elsevier, Amsterdam, 1973), Vol. 1.

[58] R. Wortmann and D. Bishop, J. Chem. Phys. **108**, 1001 (1998).

[59] M. J. Frisch, G. W. Trucks, H. B. Schlegel *et al.*, GAUSSIAN 09, Gaussian, Inc., Pittsburgh, PA, 2009.

[60] K. S. Pitzer, J. Am. Chem. Soc. **67**, 1126 (1945).

[61] R. S. Mulliken, Chem. Rev. **41**, 207 (1947).

[62] H. C. Longuet-Higgins, Q. Rev. Chem. Soc. **11**, 121 (1957).

[63] W. N. Lipscomb, *Boron Hydrides* (W. A. Benjamin, New York, 1963).

[64] E. Switkes, W. N. Lipscomb, and M. D. Newton, J. Am. Chem. Soc. **92**, 3847 (1970).

[65] I. R. Epstein, D. S. Marynick, and W. N. Lipscomb, J. Am. Chem. Soc. **95**, 1760 (1973).

[66] D. A. Kleier, T. A. Halgren, and W. N. Lipscomb, J. Chem. Phys. **61**, 3905 (1974).

[67] S. Yamabe, T. Minato, H. Fujimoto, and K. Fukui, Theor. Chim. Acta **32**, 187 (1974).

[68] W. N. Lipscomb, Science **196**, 1047 (1977).

[69] R. F. W. Bader, S. G. Anderson, and A. J. Duke, J. Am. Chem. Soc. **101**, 1389 (1979).

[70] J. F. Stanton, R. J. Bartlett, and W. N. Lipscomb, Chem. Phys. Lett. **138**, 525 (1987).

[71] M. L. McKee, J. Am. Chem. Soc. **112**, 6753 (1990).

[72] M. Sironi, M. Raimondi, D. L. Cooper, and J. Gerratt, J. Phys. Chem. **95**, 10617 (1991).

[73] J. Cioslowki and M. L. McKee, J. Phys. Chem. **96**, 9264 (1992).

[74] R. F. Bader and D. A. Legare, Can. J. Chem. **70**, 657 (1992).

[75] H. Hohenberg and W. Kohn, Phys. Rev. **136**, B864 (1964).

[76] W. Kohn and L. J. Sham, Phys. Rev. **140**, A1133 (1965).

[77] R. G. Parr and W. Yang, *Density-Functional Theory of Atoms and Molecules* (Oxford University Press, Oxford, 1989).

[78] Y. Zhao and D. G. Truhlar, Theor. Chem. Acc. **120**, 215 (2008).

[79] A. D. McLean and G. S. Chandler, J. Chem. Phys. **72**, 5639 (1980); T. Clark, J. Chardrasekhar, G. W. Spitznagel, and P. v. R. Schleyer, J. Comp. Chem. **4**, 294 (1983); M. J. Frisch, J. A. Pople, and J. S. Binkley, J. Chem. Phys. **80**, 3265 (1984).

[80] Within the Born-Oppenheimer approximation, the effect of the pressure on the molecular properties may be analyzed according a suitable classification scheme already adopted to study the effects of the solvent and others external agents on molecular properties, at standard conditions of pressure.[5,6] This scheme classifies the effects as "direct" and "indirect." On one hand, direct effects correspond to the changes induced by the perturbation on the solute electron distribution and on the various electronic response properties, all evaluated at a fixed geometry (i.e., at a fixed point of the PES); on the other hand, indirect effects correspond to the changes into the same molecular properties due to the influence of the external agent on the topology of potential energy surface PES of the molecular system. This influence on the PES may be of two types, corresponding, respectively, to the *relaxation* of the local minima of the PES (i.e., the shift of the equilibrium geometry), and to changes in the local *curvature* of the PES. Therefore, the indirect effects may be further analyzed in terms of "relaxation" a "curvature" contributions, which may be rigorously described in terms of suitable QM molecular response functions.

[81] A. Bondi, J. Phys. Chem. **68**, 441 (1964).

[82] M. Mantina, A. C. Chamberlin, R. Valero, C. J. Cramer, and D. G. Truhlar, J. Phys. Chem. A **113**, 5806 (2009).

[83] M. Pravica, Y. Shen, Z. Quine, E. Romano, and D. Hartnett, J. Phys. Chem. B **111**, 4103 (2007).

[84] R. Le Sar, Phys. Rev. B **28**, 6812 (1983).

[85] D. Begue, C. Pouchan, J. C. Guillemin, and A. Benidar, Theor. Chem. Acc. **131**, 1122 (2012).

[86] R. A. Baudet, *Advances in Boron and the Boranes: The Molecular Structures of Boranes and Carboranes* (VCH, New York, 1988).

[87] H. Hellmann, *Einfhrung in Die Quantenchemie* (Franz Deuticke, Leipzig, 1937), p. 285.

[88] R. Feynman, Phys. Rev. **56**, 340 (1939).

[89] H. Nakatsuji, J. Am. Chem. Soc. **95**, 345 (1973).

[90] J. Tomasi, G. Alagona, R. Bonacccorsi, C. Ghio, and R. Cammi, *Semiclassical Interpretation of Intramolecular Interactions*, Theoretical Models of Chemical Bonding Vol. 3, edited by Z. B. Maksić (Springer-Verlag, Berlin, 1991).

[91] Y. Honda and H. Nakatsuji, Chem. Phys. Lett. **293**, 230 (1998).

[92] C. Ghio, E. Scrocco, and J. Tomasi, Theor. Chim. Acta **56**, 61 (1980).

[93] G. Alagona and J. Tomasi, J. Mol. Struct.: THEOCHEM **91**, 263 (1893).

[94] R. Bonaccorsi, C. Ghio, and J. Tomasi, Int. Quantum Chem. **26**, 637 (1984).

[95] G. Alagona, R. Bonaccorsi, C. Ghio, and J. Tomasi, Pure Appl. Chem. **60**, 231 (1988).

[96]G. Alagona, R. Cammi, C. Ghio, and J. Tomasi, Theor. Chim. Acta **85**, 167 (1993).
[97]See supplementary material at http://dx.doi.org/10.1063/1.4757285 for Table S1—amount of the electronic charge, Q_{out} (in -*e*) lying outside of the cavity hosting diborane as a function of the cavity scaling factor *f* and of the pressure, *p* (in GPa); Table S2—the energy gradients $G_{e-r}^{Q_i}$ of diborane, as computed at the PCM/M062X/6-311++G(d,p) level with the step barrier potential $V_0(6)$ and the harmonic vibrational frequencies of diborane as a function of the pressure, and computed at the at the PCM/M062X/6-311++G(d,p) level using the softest repulsive step potential $V_0(3)$; Table S3—harmonic vibrational frequencies of diborane as function of the pressure, as computed with the barrier potential $V_0(3)$; Table S4—the harmonic force constants k_i of diborane in gas phase and at the M062X/6-311++G(d,p) level and the harmonic force constants $\tilde{k}_i$ of diborane as a function of the pressure, and computed at the PCM/M062X/6-311++G(d,p) level using the repulsive step potential $V_0(6)$; Table S5—the harmonic force constants k_i of diborane as a fucntion of the pressure, and computed at the PCM/M062X/6-311++G(d,p) level using the repulsive step potential $V_0(6)$ and the equilibrium geometry in gas phase; and Table S6—selected cubic force constants g_{iij} of diborane in gas phase and at the M062X/6-311++G(d,p) level.
[98]M. Shen and H. F. Schaefer III, J. Chem. Phys. **96**, 2868 (1991).
[99]V. Barone, L. Orlandini, and C. Adamo, J. Phys. Chem. **98**, 13185 (1994).
[100]A. Vijay and D. N. Sathyanarayana, J. Mol. Struct. **351**, 215 (1995).
[101]F. R. Bennet and J. P. Connelly, J. Phys. Chem. **100**, 9308 (1996).
[102]R. L. Sams, T. A. Blake, S. W. Sharpe, J.-M. Flaud, and W. J. Lafferty, J. Mol. Spectrosc. **191**, 331 (1998).
[103]J. F. Stanton and J. Gauss, J. Chem. Phys. **108**, 9218 (1998).
[104]P. Ravinder and V. Subramanian, J. Phys. Chem. A **114**, 5565 (2010).
[105]J. L. Duncan, D. C. McKean, I. Torto, and G. D. Nivellini, J. Mol. Spectrosc. **85**, 16 (1981); J. L. Duncan, J. Harper, E. Hamilton, and G. D. Nivellini, *ibid.* **102**, 416 (1983).
[106]D. Papousek and M. R. Aliev, *Molecular Vibrational-Rotational Spectra* (Elsevier, Amsterdam, 1982); F. Egidi, V. Barone, J. Bloino, and C. Cappelli, J. Chem. Theory Comput. **8**, 585 (2012).
[107]The partition of the pressure effects on the harmonic force constant into "curvature" and "relaxation" contributions, has a direct correspondence with an analogous partition introduced to describe the effects of the electric field on second and higher order molecular response functions (see Ref. 108 on this topic).
[108]J. Martí, J. L. Andrés, J. Bertrán, and M. Duran, Mol. Phys. **80**, 625 (1993); J. Martí and D. M. Bishop, J. Chem. Phys. **99**, 3860 (1993).
[109]Combining Eqs. (42) and (45), the pressure coefficient of the harmonic vibrational frequencies can be partitioned as

$$\frac{d\tilde{\nu}_i}{dp} = \left.\frac{d\tilde{\nu}_i}{dp}\right|_{cur} + \left.\frac{d\tilde{\nu}_i}{dp}\right|_{rel},$$

where the terms describing the curvature and relaxation effects of the pressure on the harmonic vibrational frequencies are given in terms of the corresponding effects on the harmonic force constants:

$$\left.\frac{d\tilde{\nu}_i}{dp}\right|_{cur} = \frac{1}{2}\left(\frac{\nu_i}{k_i}\right)\left.\frac{dk_i}{dp}\right|_{cur}$$

$$\left.\frac{d\tilde{\nu}_i}{dp}\right|_{rel} = \frac{1}{2}\left(\frac{\nu_i}{k_i}\right)\left.\frac{d\nu_i}{dp}\right|_{rel}.$$